

Supplementary Data for the manuscript

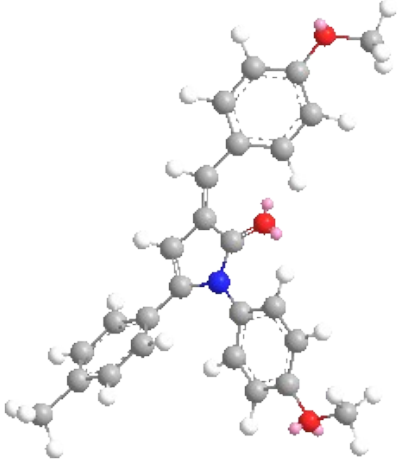
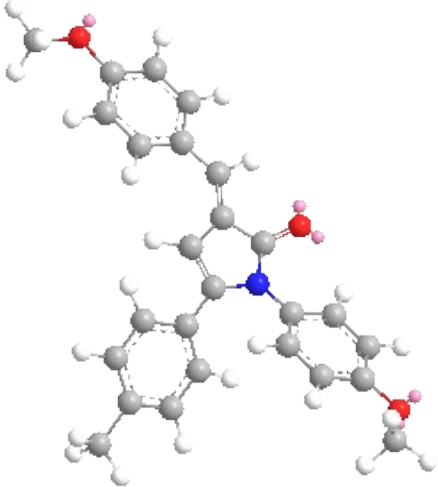
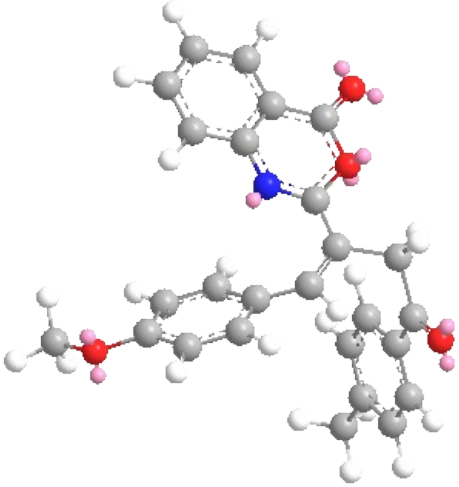
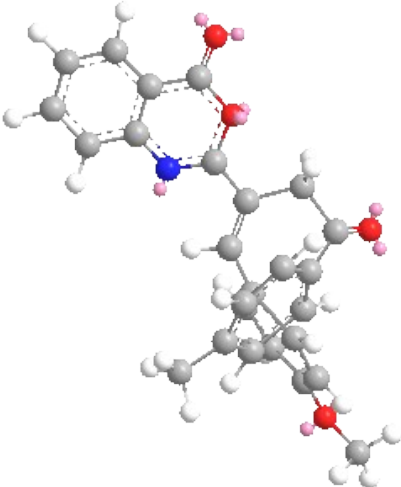
“Transformation of 3-(4-methoxybenzylidene)-5-(p-tolyl)-2(3H)-Furanone into New Nitrogen-containing Heterocyclic Candidates as Insecticidal Agents” by Nourhan M. Gad *et al.*

This file provides extended computational and physicochemical datasets supporting the main manuscript. It includes:

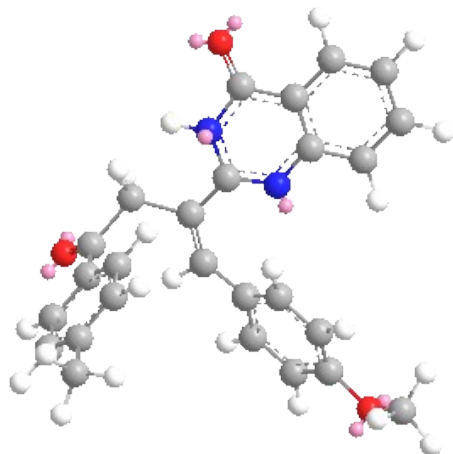
- **Table S1:** Space-model analysis of *Z/E* stereoisomers for selected compounds (**4**, **7**, **8**, and **9**). The table reports total MM2 energies (kcal/mol) and 1,4-van der Waals (VDW) interactions used to infer the preferred configuration for each compound.
- **Tables S2–S5:** Detailed residue-level docking interaction data for all synthesized compounds with AChE and Met receptors.
- **Figure S1:** Molecular dynamics (MD) results for Met–ligand systems over 100 ns, including RMSD and RMSF profiles for compound **4**, pyriproxyfen, and the redocked co-crystallized ligand (HNJ) transferred to the modeled Met PAS-B domain.
- **Figure S2:** Ligand–protein contact histograms and interaction frequency maps for Met–ligand complexes (compound **4**, pyriproxyfen, and HNJ), illustrating interaction persistence within the hormone-binding cavity across the simulation trajectory.
- **Figures S3–S9:** SwissADME analyses of the synthesized compounds, covering lipophilicity, solubility, bioavailability, and drug-likeness parameters.

These supplementary materials provide extended structural, dynamic, and pharmacokinetic characterization supporting the analyses presented in the main manuscript.

Table S1. Space-model analysis of *Z/E* stereoisomers for selected compounds (**4**, **7**, **8**, and **9**). The table reports total MM2 energies (kcal/mol) and 1,4-van der Waals (VDW) interactions used to infer the preferred configuration for each compound.

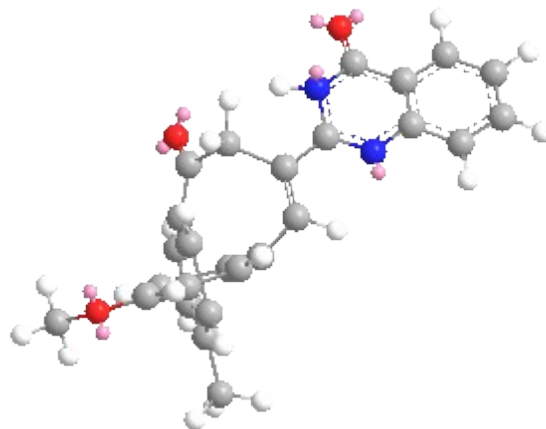
Comps.	<i>Z</i> -isomer	<i>E</i> -isomer
4	 <p data-bbox="509 947 654 978">^aE = 66.03</p> <p data-bbox="456 1024 708 1056">^b 1,4-VDW = 31.26</p>	 <p data-bbox="1138 972 1263 1003">E = 60.75</p> <p data-bbox="1084 1052 1317 1083">1,4-VDW = 31.37</p>
7	 <p data-bbox="518 1675 646 1707">E = 47.31</p> <p data-bbox="467 1755 696 1787">1,4-VDW = 33.93</p>	 <p data-bbox="1122 1682 1279 1713">E = 1092.68</p> <p data-bbox="1084 1761 1317 1793">1,4-VDW = 36.90</p>

8



E = 45.54

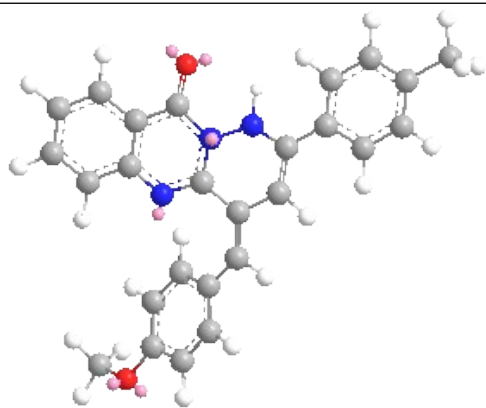
1,4-VDW = 30.23



E = 1001.50

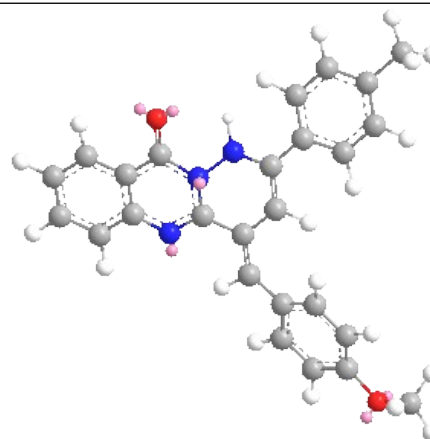
1,4-VDW = 22.22

9



E = 41.79

1,4-VDW = 37.77



E = 39.58

1,4-VDW = 37.50

^b VDW: van-der Waal interactions.

^a E: Total Energy in kcal/mol.

Table S2: Summary of molecular docking interaction data for all synthesized compounds with the acetylcholinesterase (AChE) model, including interaction types, distances, and estimated binding energies.

Compound	Ligand atom	Receptor atom	Residue	Interaction Type	Distance	E (kcal/mol)
1	O 7	CB	HIS 567 (A)	H-acceptor	3.19	-0.6
	6-ring	5-ring	TRP 212 (A)	pi-pi	4.07	
	6-ring	6-ring	TRP 212 (A)	pi-pi	4.13	
2	O 8	CB	HIS 567 (A)	H-acceptor	3.16	-0.7
	5-ring	CD2	HIS 567 (A)	pi-H	4.08	-1.5
	6-ring	5-ring	TRP 212 (A)	pi-pi	4.05	
3	6-ring	6-ring	TRP 212 (A)	pi-pi	4.06	
	C 25	OE1	GLU 326 (A)	H-donor	3.34	-0.5
	O 7	CD2	HIS 567 (A)	H-acceptor	3.44	-0.5
	O 24	OH	TYR 258 (A)	H-acceptor	3.23	-0.8
	6-ring	5-ring	TRP 212 (A)	pi-pi	4.19	
4	6-ring	6-ring	TRP 212 (A)	pi-pi	4.17	
	O 7	CB	HIS 567 (A)	H-acceptor	3.24	-0.5
	5-ring	CD2	HIS 567 (A)	pi-H	4.09	-1.6
	6-ring	5-ring	TRP 212 (A)	pi-pi	3.98	
5	6-ring	6-ring	TRP 212 (A)	pi-pi	3.83	
	O 34	CB	HIS 567 (A)	H-acceptor	3.28	-0.5
	C 52	6-ring	TRP 360 (A)	H-pi	3.78	-0.5
	5-ring	CD2	HIS 567 (A)	pi-H	4.12	-1.6
	6-ring	5-ring	TRP 212 (A)	pi-pi	3.99	
7	6-ring	6-ring	TRP 212 (A)	pi-pi	3.66	
	O 37	CA	GLY 568 (A)	H-acceptor	3.2	-0.7
	6-ring	5-ring	TRP 212 (A)	pi-pi	3.54	
8	6-ring	6-ring	TRP 212 (A)	pi-pi	3.6	
	O 38	CA	GLY 568 (A)	H-acceptor	3.18	-0.7
	6-ring	5-ring	TRP 212 (A)	pi-pi	3.62	
9	6-ring	6-ring	TRP 212 (A)	pi-pi	3.62	
	O 21	OH	TYR 249 (A)	H-acceptor	2.63	-1.3
	6-ring	CA	GLY 246 (A)	pi-H	3.76	-1.7
10	6-ring	5-ring	TRP 212 (A)	pi-pi	4.09	
	O 9	CD2	HIS 567 (A)	H-acceptor	3.34	-0.5
11	6-ring	CB	HIS 567 (A)	pi-H	4.48	-0.7
	S 8	OH	TYR 258 (A)	H-acceptor	3.03	-2.7
	6-ring	NE2	HIS 567 (A)	pi-cation	4.01	-0.5
12	6-ring	5-ring	TRP 212 (A)	pi-pi	4.34	
	6-ring	NE2	HIS 567 (A)	pi-cation	3.99	-0.5
	6-ring	5-ring	TRP 212 (A)	pi-pi	4.33	

13	O 7	CB	HIS 567 (A)	H-acceptor	3.17	-0.7
	5-ring	CD2	HIS 567 (A)	pi-H	4.03	-0.9
	6-ring	5-ring	TRP 212 (A)	pi-pi	4	
	6-ring	6-ring	TRP 212 (A)	pi-pi	3.93	
14	6-ring	CD2	HIS 567 (A)	pi-H	4.27	-0.6
Chlorpyrifos	S 4	N	GLY 247 (A)	H-acceptor	4.43	-0.5
	S 4	CB	SER 327 (A)	H-acceptor	3.61	-0.9
	S 4	NE2	HIS 567 (A)	H-acceptor	4.45	-3.2
	C 11	5-ring	TRP 212 (A)	H-pi	3.74	-0.6
Native CCL	C07 8	OE1	GLU 326 (A)	H-donor	3.5	-0.5
	O12 15	N	GLY 247 (A)	H-acceptor	2.77	-1.8
Redocked CCL	O12 15	N	GLY 247 (A)	H-acceptor	2.88	-0.9
	O12 15	N	ALA 328 (A)	H-acceptor	3.31	-0.7
	5-ring	CD2	HIS 567 (A)	pi-H	4.02	-0.8

Table S3: Two-dimensional interaction diagrams illustrating the binding orientations and contact patterns of the synthesized compounds within the AChE active site obtained from docking analysis

1	2
3	4
5	7

8	9
10	11
12	13
14	Chlorpyrifos 7S

Native Cocrystallized ligand	Redocked Cocrystallized Ligand

Table S4: Summary of molecular docking interaction data for the synthesized compounds with the Methoprene-tolerant (Met) receptor model, including interaction types, distances, and binding-energy estimates.

Compound	Ligand atom	Receptor atom	Residue	Interaction Type	Distance	E (kcal/mol)	
1	C 25	5-ring	HIS 23 (B)	H-pi	4.1	-0.6	
		6-ring	SG	CYS 115 (B)	pi-H	4.9	-0.5
2	C 33	5-ring	HIS 23 (B)	H-pi	4.09	-0.5	
		5-ring	CG2	THR 21 (B)	pi-H	4.08	-1.1
		6-ring	SG	CYS 115 (B)	pi-H	4.92	-0.5
3	C 35	5-ring	HIS 23 (B)	H-pi	3.69	-0.6	
4	C 40	NE2	HIS 23 (B)	H-donor	3.29	-0.6	
5	C 38	NE2	HIS 23 (B)	H-donor	3.28	-0.6	
7	O 15	SD	MET 56 (B)	H-donor	3.61	-0.9	
	C 16	5-ring	HIS 23 (B)	H-pi	3.67	-1.6	
8	C 28	NE2	HIS 23 (B)	H-donor	3.21	-0.6	
8	N 4	SG	CYS 115 (B)	H-acceptor	3.59	-0.5	
9	C 17	5-ring	HIS 23 (B)	H-pi	3.67	-0.7	
10	N 7	OD1	ASN 117 (B)	H-donor	2.84	-2.3	
	C 28	5-ring	HIS 23 (B)	H-pi	4.17	-0.5	
		6-ring	CG2	THR 21 (B)	pi-H	4.04	-0.6
11	S 8	CA	GLY 27 (B)	H-acceptor	3.15	-1.1	
	S 8	CG	PRO 52 (B)	H-acceptor	3.89	-0.7	
	C 23	5-ring	HIS 23 (B)	H-pi	3.89	-0.5	
12	C 22	5-ring	HIS 23 (B)	H-pi	4.01	-1	
		6-ring	5-ring	HIS 23 (B)	pi-pi	4.4	
13	C 33	NE2	HIS 23 (B)	H-donor	3.26	-0.6	
		5-ring	SG	CYS 115 (B)	pi-H	4.48	-0.8
14	N 7	O	PRO 52 (B)	H-donor	3.2	-1.7	
	C 39	NE2	HIS 23 (B)	H-donor	3.23	-0.5	
Pyriproxyfen	6-ring	CD1	LEU 68 (B)	pi-H	3.94	-0.6	
	6-ring	5-ring	HIS 23 (B)	pi-pi	4.37		
Native CCL			No Detected Interactions				
Redocked CCL	N 25	SD	MET 56 (B)	H-donor	3.2	-1.4	
	O 8	CE1	HIS 23 (B)	H-acceptor	3.35	-0.6	

Table S5: Two-dimensional interaction diagrams showing the binding orientations and interaction patterns of the synthesized compounds within the Met receptor binding cavity as predicted by docking

1	2
3	4
5	7

8	9
10	11
12	13

14	pyriproxyfen
Native Cocrystallized ligand	Redocked Cocrystallized Ligand

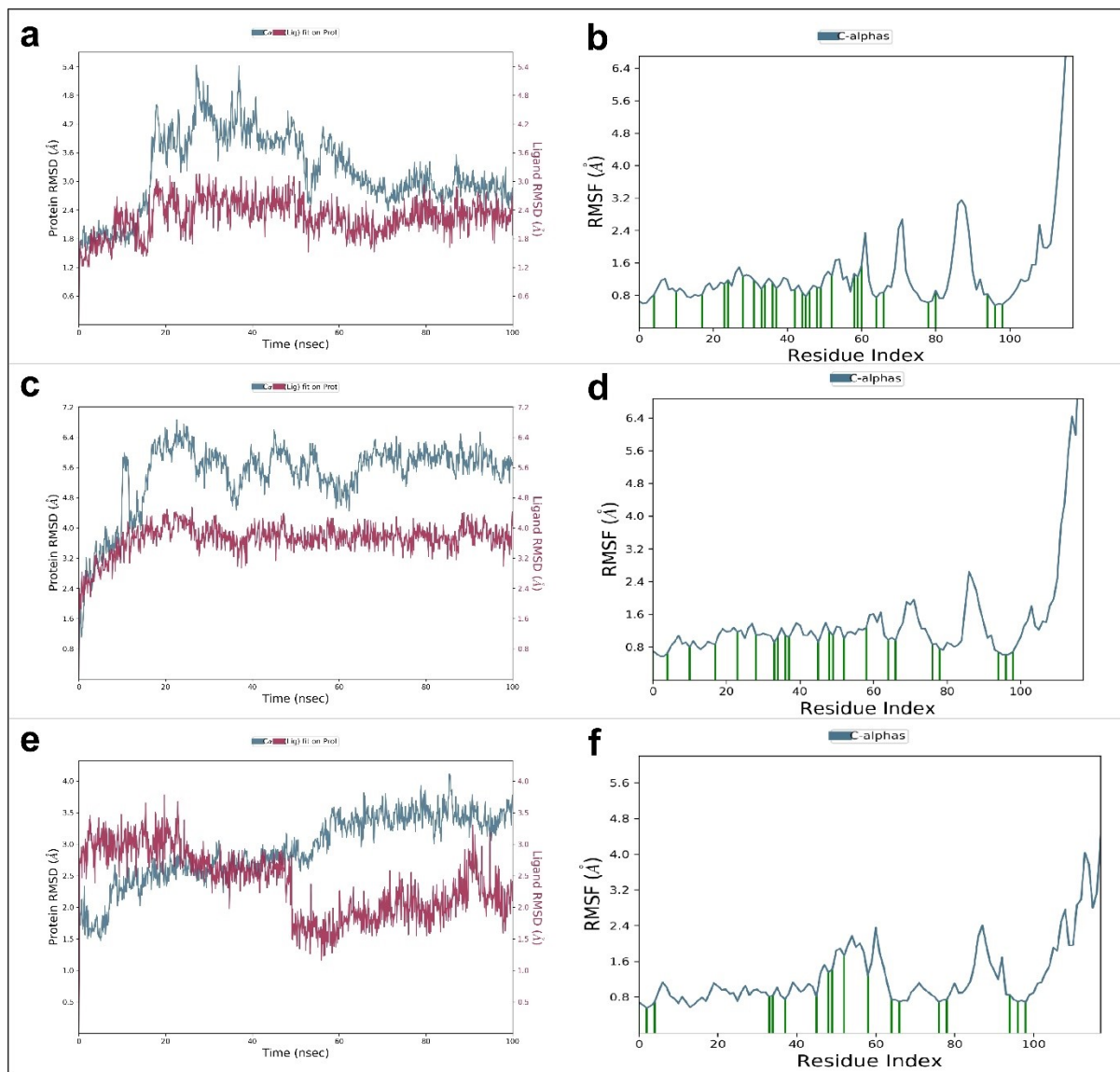


Fig. S1: MD results for Met–ligand systems over 100 ns: (a) RMSD of compound 4; (b) RMSF of compound 4; (c) RMSD of pyriproxyfen; (d) RMSF of pyriproxyfen; (e) RMSD of the redocked co-crystallized ligand (HNJ) transferred to the modeled Met PAS-B domain; (f) RMSF of the same ligand.

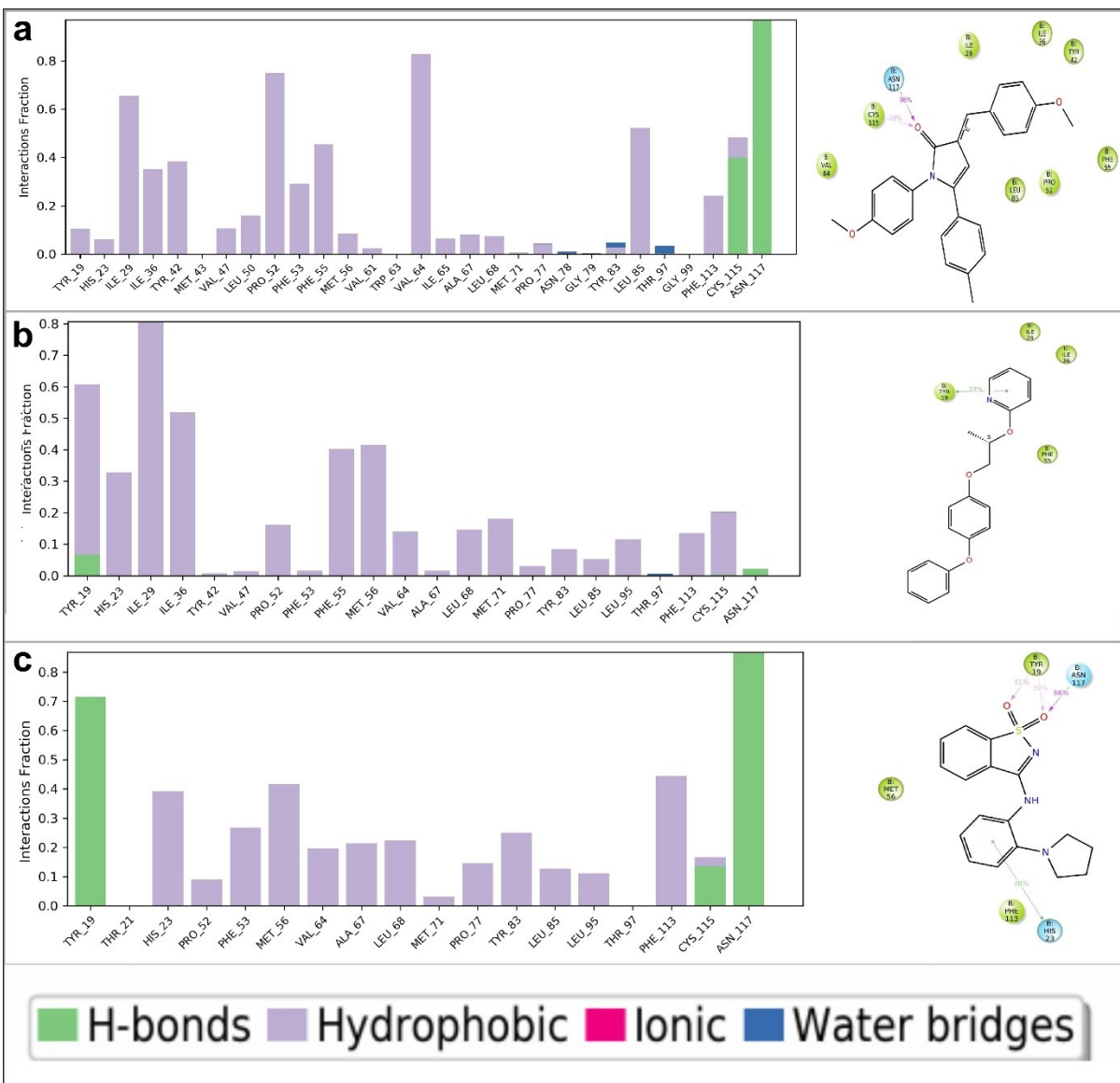


Fig. S2: Ligand–protein contact histograms and interaction frequency maps for Met–ligand complexes: (a) compound **4**; (b) pyriproxyfen; and (c) the redocked co-crystallized ligand (HNJ), showing consistent contacts with residues within the hormone-binding pocket across the simulation trajectory.

Fig. S3

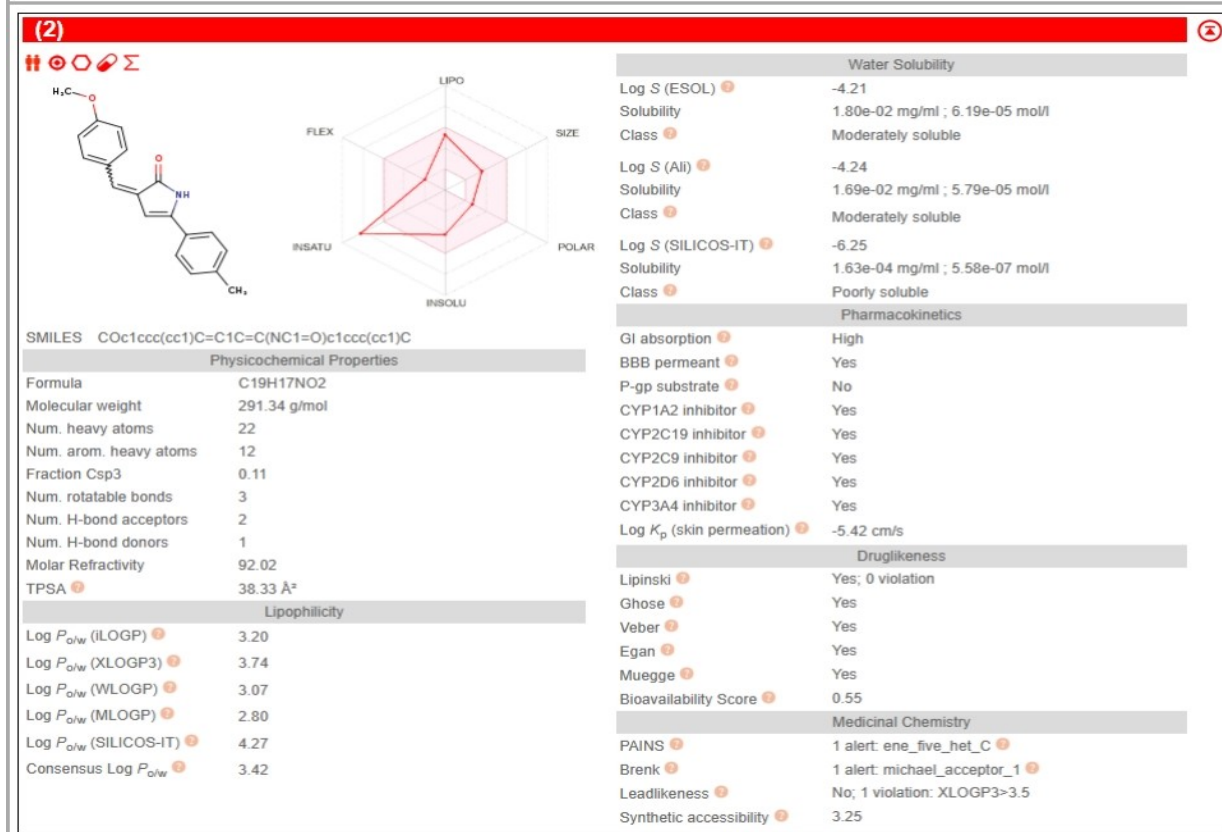
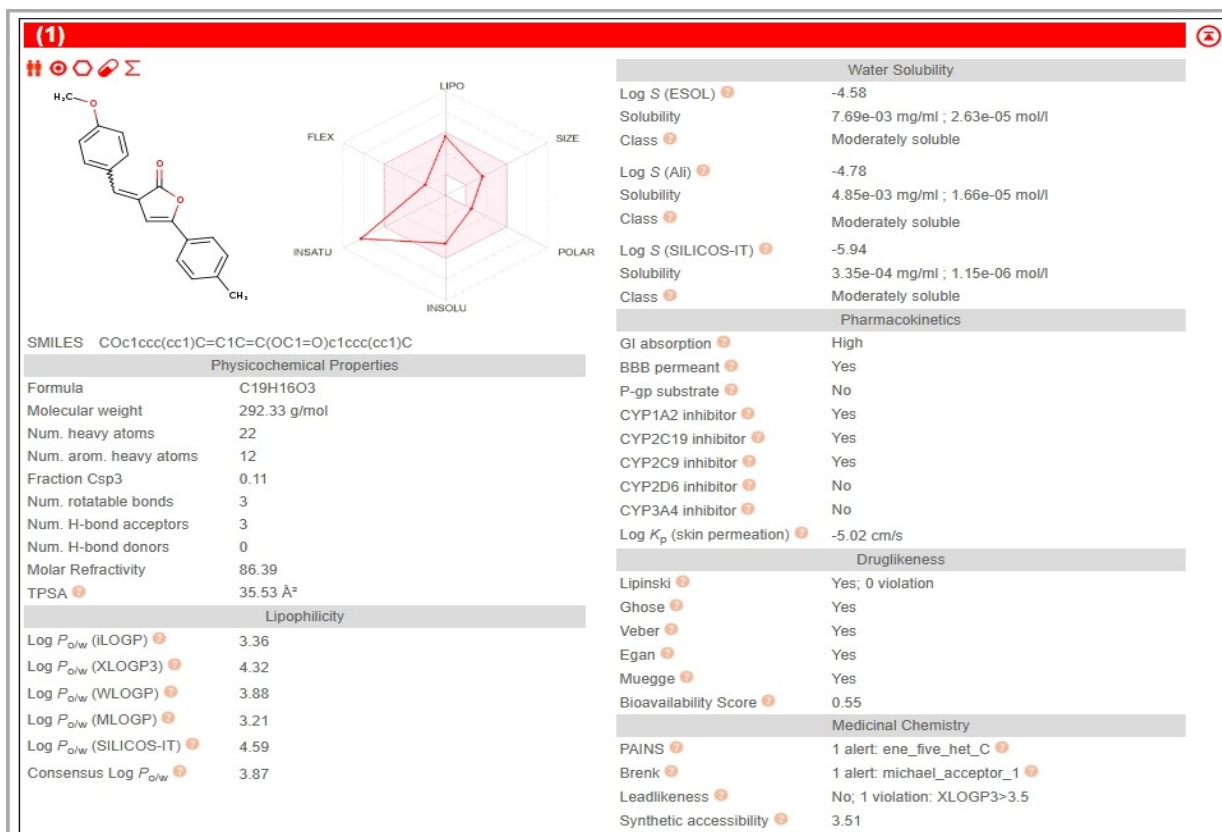


Fig.S4

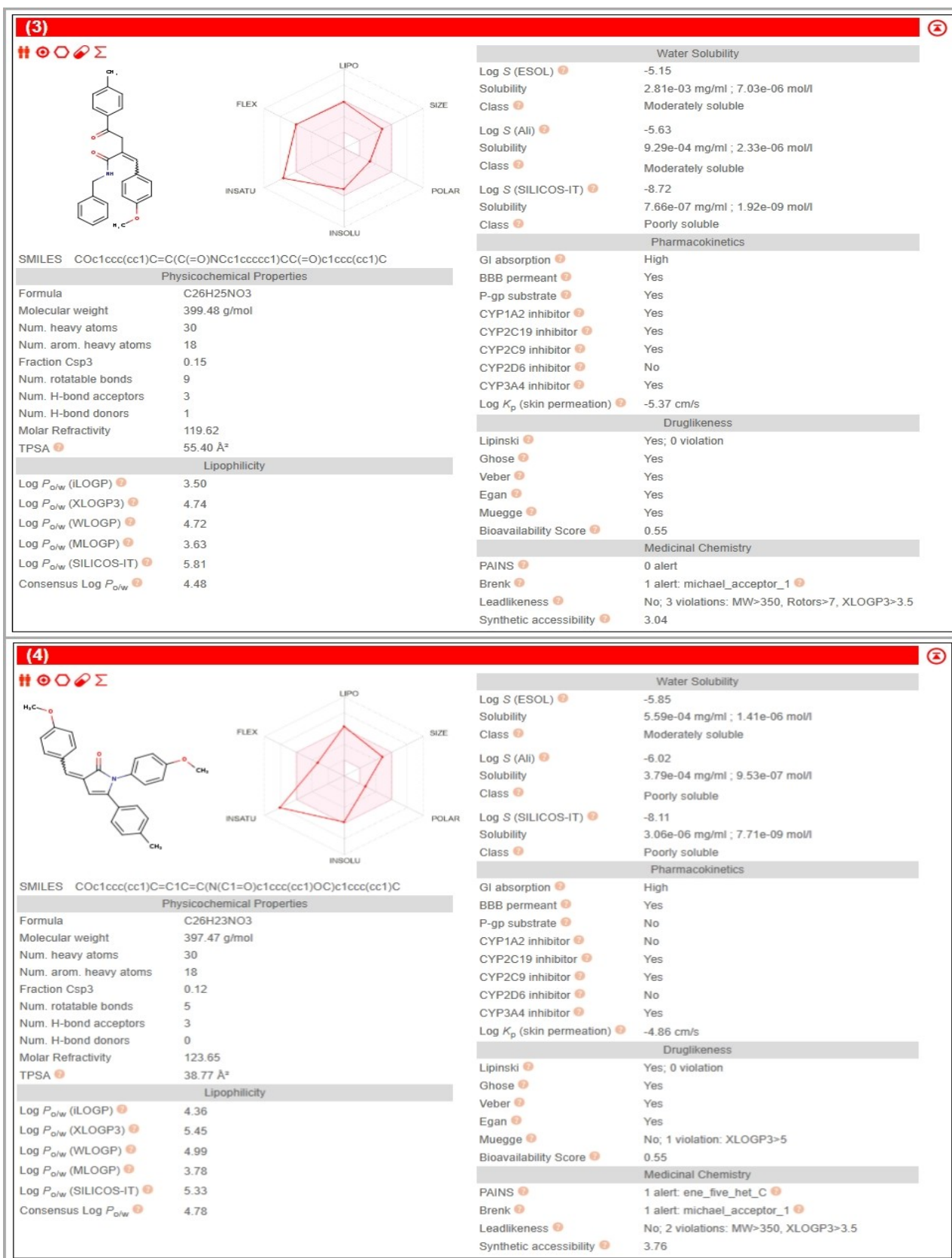


Fig. S5

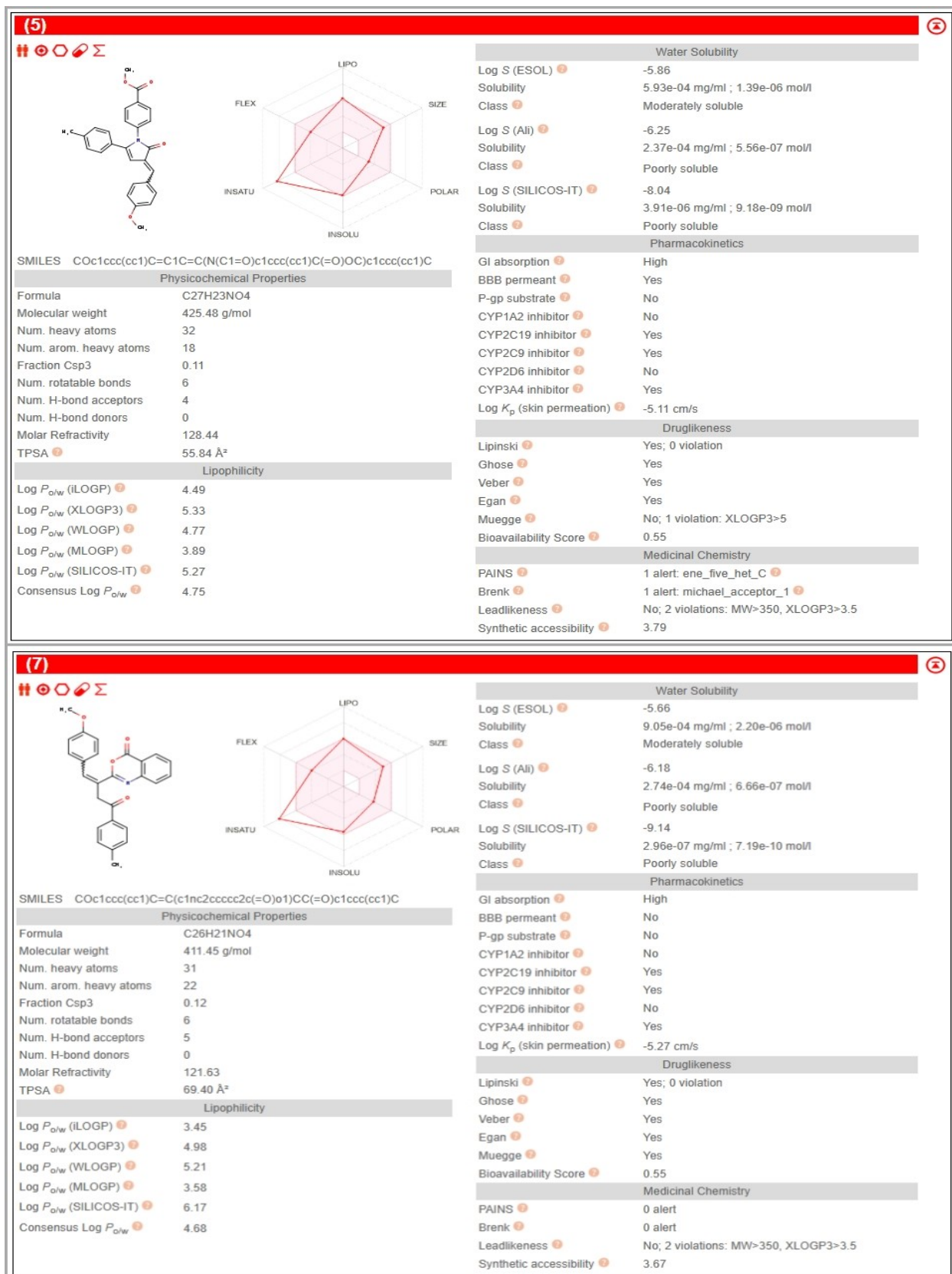


Fig. S6

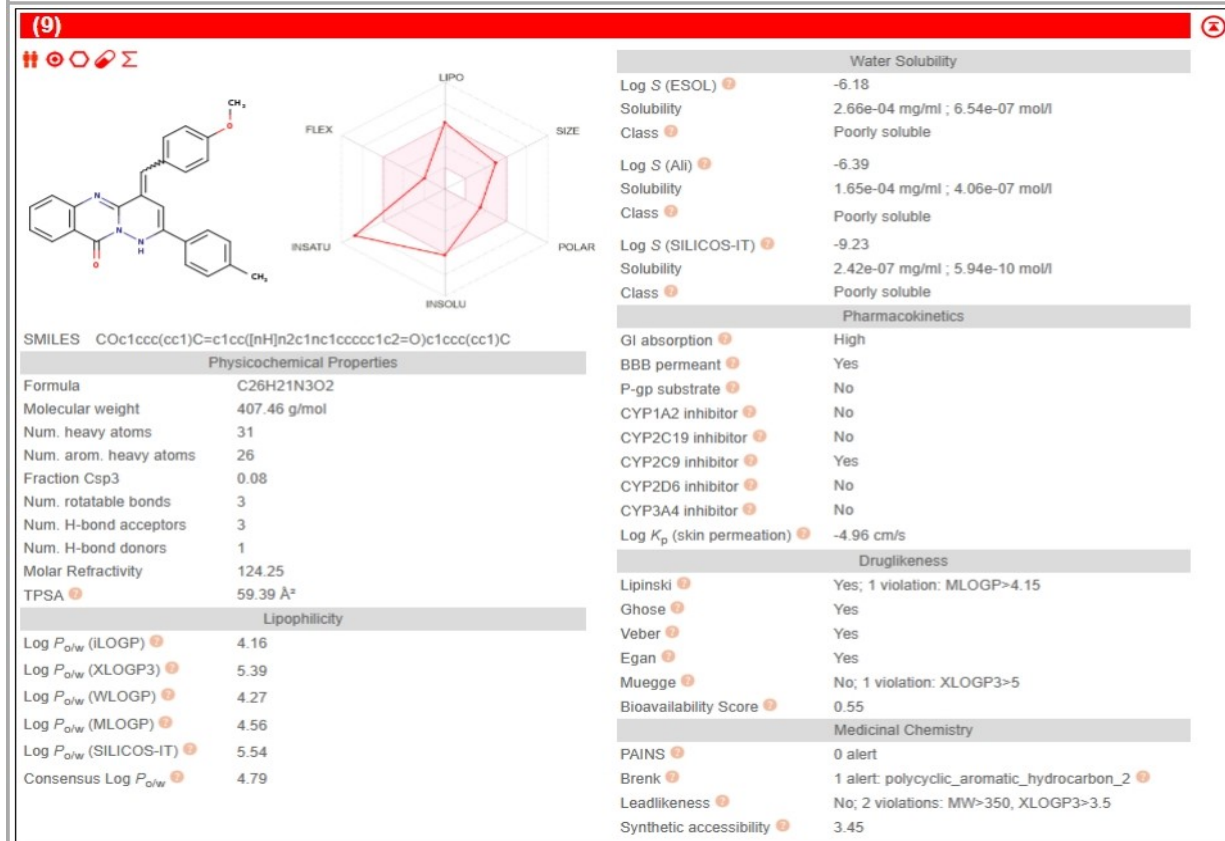
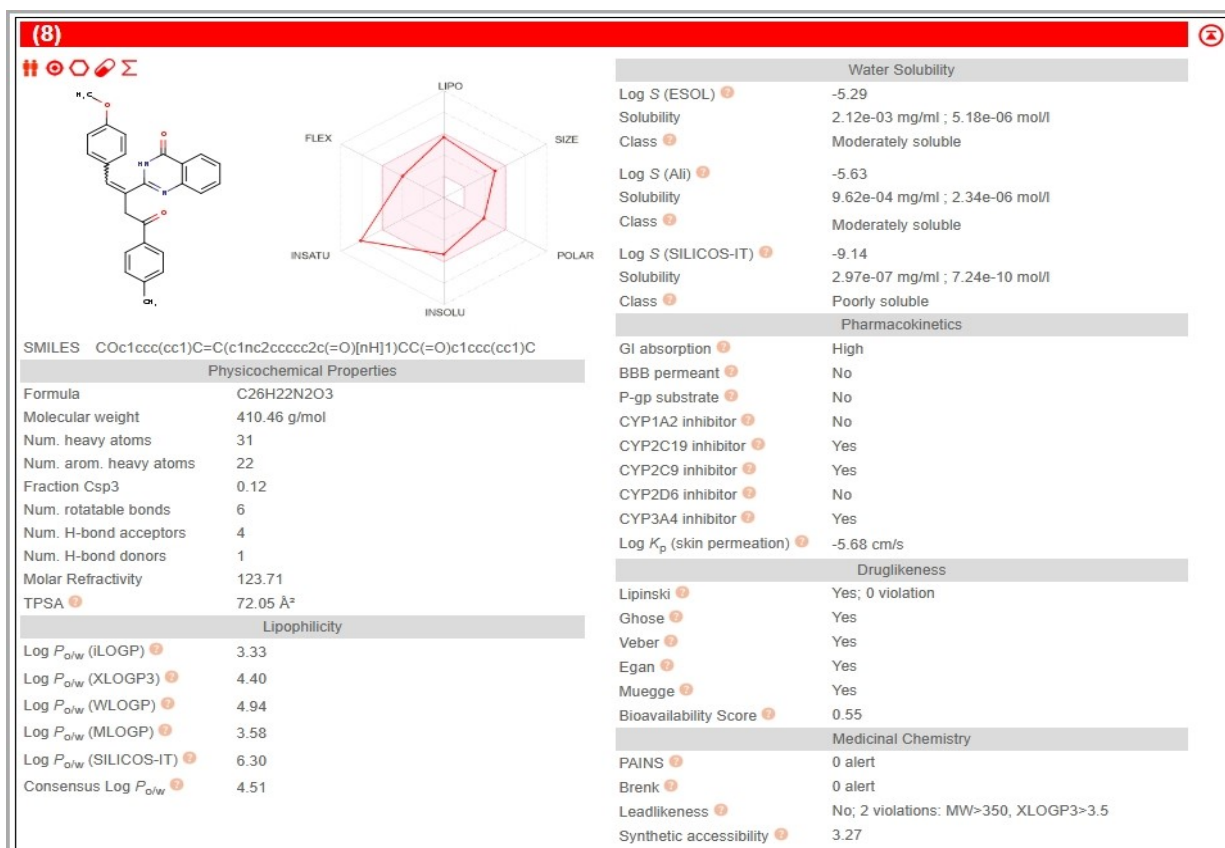


Fig. S7

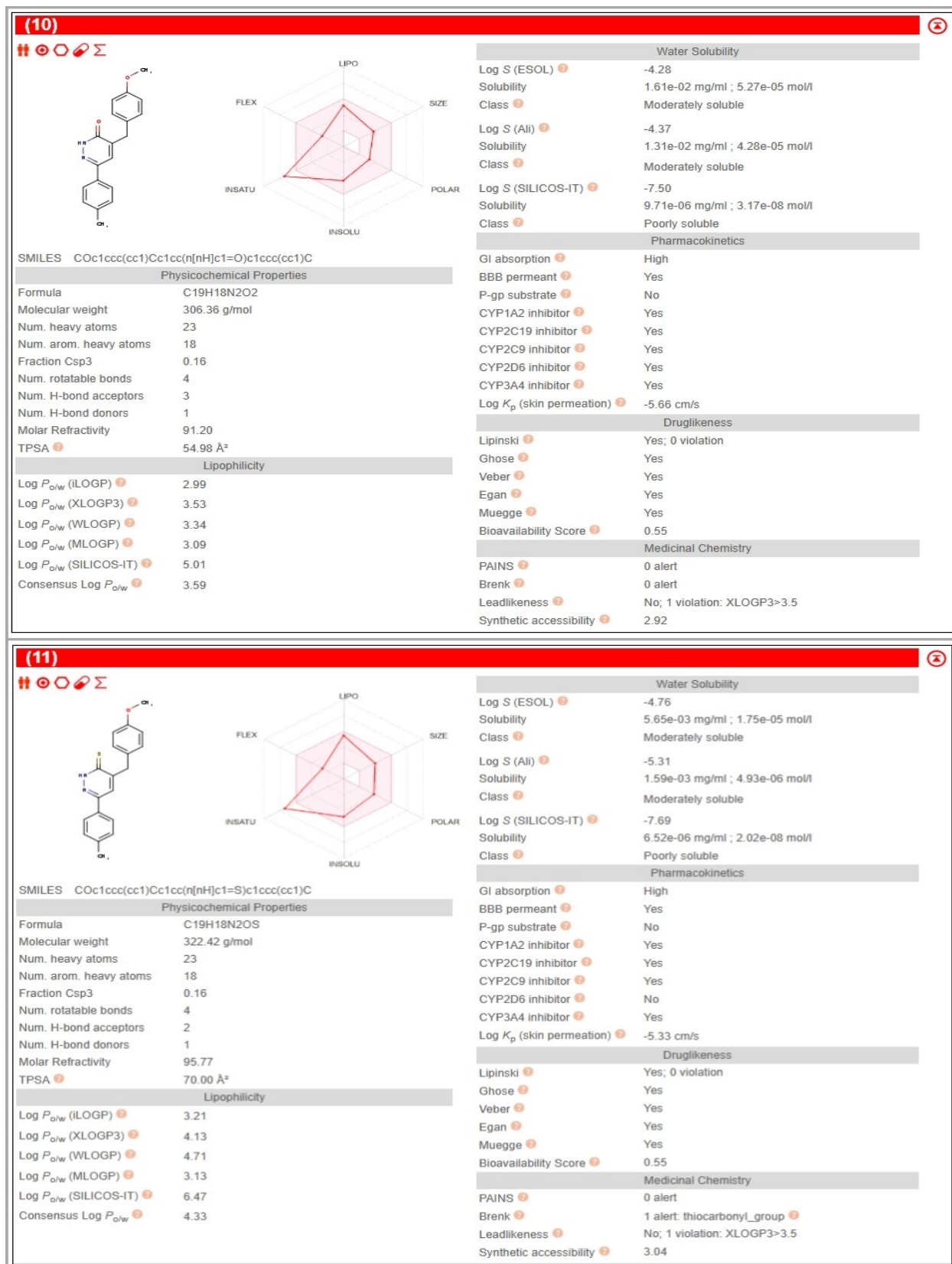


Fig. S8

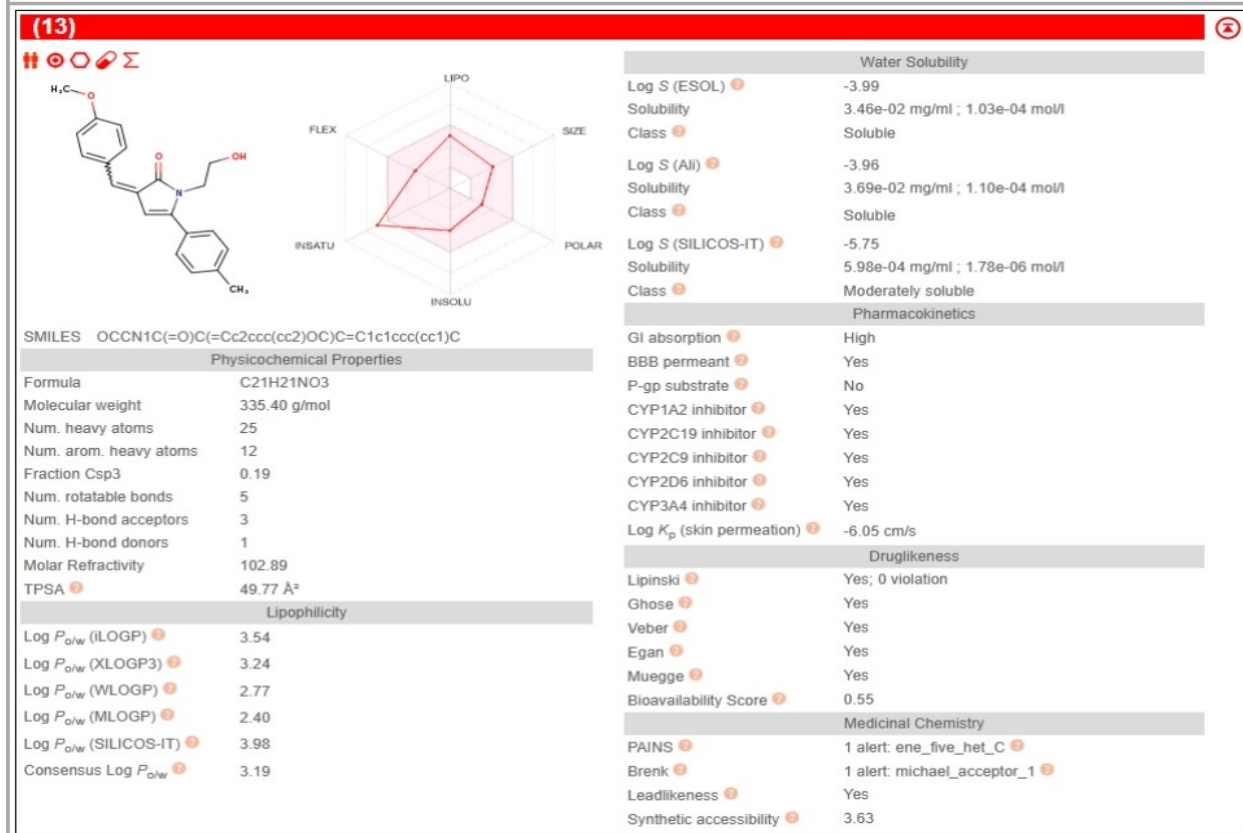
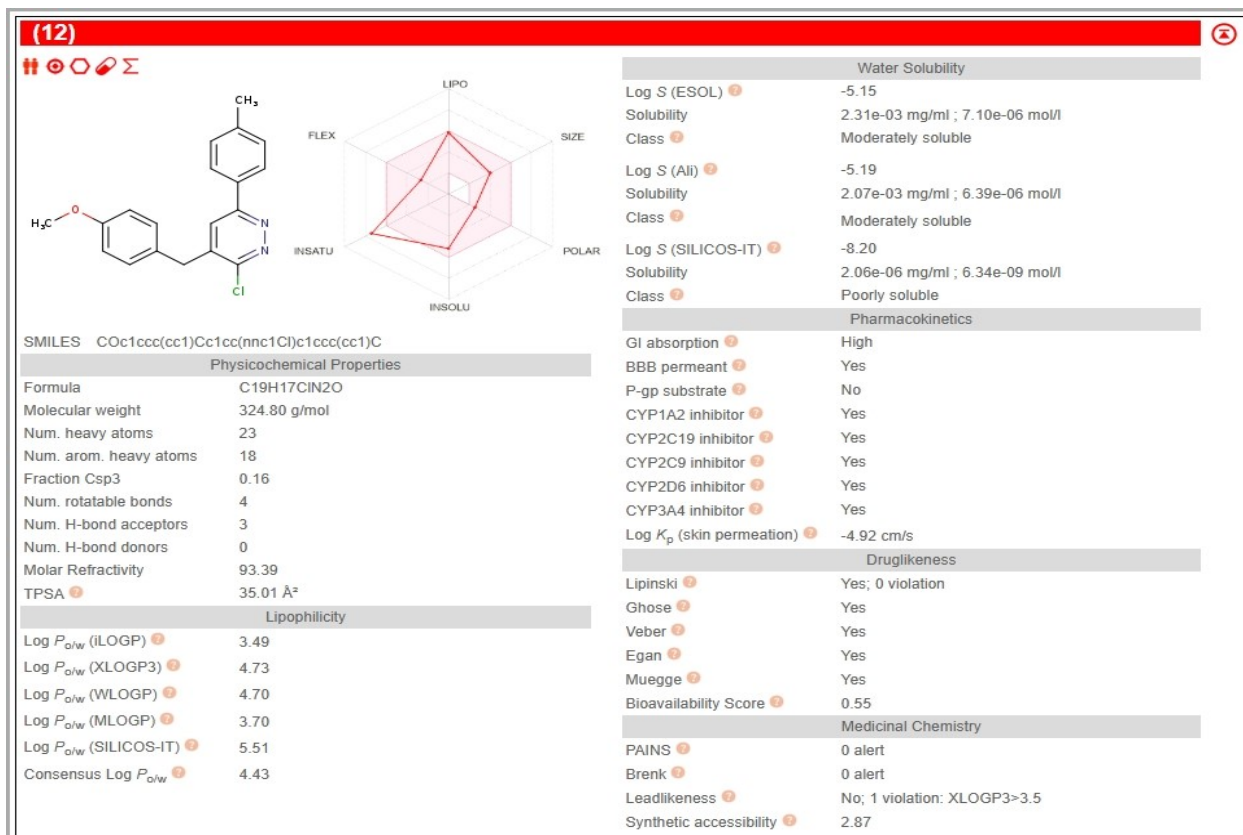


Fig.S9

